α7 Nicotinic Acetylcholine Receptor Regulates the Function and Viability of L Cells

Dawei Wang,[1,2]* Qinghe Meng,[2]* Colin A. Leech,[2] Natesh Yepuri,[2] Linlin Zhang,[2] George G. Holz,[3,4] Chunting Wang,[5] and Robert N. Cooney[2]

[1]Department of Intensive Care Unit, Zhongnan Hospital of Wuhan University, Wuhan, Hubei 430071, China; [2]Department of Surgery, SUNY Upstate Medical University, Syracuse, New York 13210; [3]Department of Medicine, SUNY Upstate Medical University, Syracuse, New York 13210; [4]Department of Pharmacology, SUNY Upstate Medical University, Syracuse, New York 13210; and [5]Department of Critical Care Medicine, Shandong Provincial Hospital, Shandong University, Jinan 250101, Shandong Province, China

Enteroendocrine L cells secrete the incretin hormone glucagon-like peptide-1 (GLP-1), and they also express the α7 nicotinic acetylcholine receptor (α7nAChR), which may regulate GLP-1 secretion. Here, GTS-21, a selective α7nAChR agonist, was used to examine the effect of α7nAChR activation in L-cell lines, mouse intestinal primary cell cultures, and C57BL/6 mice. GTS-21 stimulated GLP-1 secretion *in vitro*, and this effect was attenuated by an α7nAChR antagonist or by α7nAChR-specific small interfering RNA. Under *in vitro* cell culture conditions of glucotoxicity, GTS-21 restored GLP-1 secretion and improved L-cell viability while also acting *in vivo* to raise levels of circulating GLP-1 in mice. To assess potential signaling mechanisms underlying these actions of GTS-21, we first monitored Ca^{2+}, cAMP, and phosphatidylinositol 3-kinase (PI3K) activity. As expected for a GLP-1 secretagogue promoting Ca^{2+} influx through α7nAChR cation channels, $[Ca^{2+}]_i$ increased in response to GTS-21, but $[cAMP]_i$ was unchanged. Surprisingly, pharmacological inhibition of growth factor signaling pathways revealed that GTS-21 also acts on the PI3K–protein kinase B–mammalian target of rapamycin pathway to promote L-cell viability. Moreover, the Ca^{2+} chelator BAPTA-AM counteracted GTS-21–stimulated PI3K activity, thereby indicating unexpected crosstalk of L-cell Ca^{2+} and growth factor signaling pathways. Collectively, these data demonstrate that α7nAChR activation enhances GLP-1 secretion by increasing levels of cytosolic Ca^{2+} while also revealing Ca^{2+}- and PI3K-dependent processes of α7nAChR activation that promote L-cell survival. **(*Endocrinology* 159: 3132–3142, 2018)**

Glucagon-like peptide-1 (GLP-1) is an incretin hormone that is produced mainly by enteroendocrine L cells lining the intestinal mucosa (1). GLP-1 binds its G protein–coupled receptors (GLP-1Rs) on pancreatic β cells to stimulate insulin secretion (2), and it also acts at the GLP-1R on brainstem and vagal afferent sensory neurons to control energy homeostasis (3, 4). Circulating GLP-1 has a short half-life because it is rapidly degraded by the enzyme dipeptidyl peptidase-4. Therefore, drugs that mimic the action of native GLP-1 or that inhibit GLP-1 degradation have become important therapies for type 2 diabetes mellitus (T2DM) (5, 6).

L cells are located predominantly in the distal ileum and colon. L-cell function is influenced by luminal nutrients, hormones, inflammation, and vagal nerve regulation (7). With apical processes facing the gut lumen, L cells directly sense nutrient levels in the intestine. Nutrient ingestion results in a biphasic pattern of GLP-1 secretion (8). The initial secretion is mediated through a neuro/endocrine pathway, which involves vagal activity and the secretion of gastric inhibitory polypeptide (9, 10).

ISSN Online 1945-7170

Received 3 May 2018. Accepted 2 July 2018.
First Published Online 9 July 2018

*These authors contributed equally to this study.

Abbreviations: Akt, protein kinase B; FBS, fetal bovine serum; GLP-1, glucagon-like peptide-1; GLP-1R, glucagon-like peptide-1 receptor; JAK2, Janus kinase 2; mTOR, mammalian target of rapamycin; MTT, 3-[4,5-dimethylthiazol-2-yl]-2,5 diphenyl tetrazolium bromide; pen-strep, penicillin and streptomycin; PI3K, phosphatidylinositol 3-kinase; siRNA, small interfering RNA; T2DM, type 2 diabetes mellitus; α7nAChR, α7 nicotinic acetylcholine receptor; α-BgTX, α-bungarotoxin.

Delayed secretion involves the direct detection of luminal nutrients by L cells (11). L cells are generated from stem cells at the base of intestinal crypts, and L-cell number can be augmented by dietary fiber, short-chain fatty acids, polysaccharides, and the gut microbiota (12–14). However, L-cell function and viability are negatively influenced by glucotoxicity and lipotoxicity, both factors that are implicated in the pathogenesis of T2DM (15–17). On the basis of current knowledge, agents that stimulate GLP-1 secretion by promoting L-cell differentiation and/or by increasing L-cell numbers likely represent promising therapies to improve glycemic control in T2DM (18, 19).

The α7 nicotinic acetylcholine receptor (α7nAChR) forms a Ca^{2+}-permeant pentameric ligand-gated cation channel (20). These α7 receptors are widely expressed in neuronal and nonneuronal cells, and several α7nAChR-selective agonists (*e.g.,* GTS-21, PNU-282987, and TC-5619) are currently being tested in clinical trials of neurologic and psychiatric diseases (21). Although acetylcholine released from vagal efferent nerves is known to regulate GLP-1 secretion through activation of L-cell muscarinic receptors (22), α7nAChR expression was recently described in the enteroendocrine STC-1 cell line (23). However, the potential role of these nicotinic receptors in the regulation of GLP-1 secretion or L-cell viability is unknown. Thus, to investigate α7nAChR signaling in the context of enteroendocrine cell function, we took advantage of intestinal cell lines of mouse (GLUTag, STC-1) or human (NCI-H716) origin that are widely used to study mechanisms controlling the secretion of GLP-1. Although none of these cell lines represents a perfect model of native L cells (24), the GLUTag cells appear to be quite well differentiated, and they recapitulate the responsiveness of primary intestinal cell cultures to physiological and pharmacological GLP-1 secretagogues (25, 26).

Here, we report α7nAChR regulation of L-cell GLP-1 secretion and L-cell viability, as studied using not only GLUTag, NCI-H716, and STC-1 cells but also mouse intestinal primary cell cultures. First, we confirmed α7nAChR expression in GLUTag, NCI-H716, and STC-1 cells and L cells of mouse intestinal primary cell cultures and small intestine. Next, we used GTS-21, an α7nAChR-selective agonist, to demonstrate the effects of α7nAChR activation on GLP-1 secretion and L-cell viability in the absence or presence of glucotoxicity. Using selective pharmacological inhibitors, we also examined the role of Ca^{2+}, cAMP, and the phosphatidylinositol 3-kinase (PI3K)–protein kinase B (Akt)–mammalian target of rapamycin (mTOR) pathways in regulating GLP-1 secretion and L-cell viability. Finally, we administered GTS-21 by intraperitoneal injection to demonstrate its *in vivo* GLP-1 secretagogue action. Collectively, these results demonstrate that under conditions of *in vitro* glucotoxicity, GTS-21 restores GLP-1 secretion and L-cell viability while also acting *in vivo* to raise circulating levels of GLP-1.

Materials and Methods

Animals and reagents

C57BL/6 mice (5 to 8 weeks old) were obtained from Charles River Laboratories (Wilmington, MA), and gut tissue for this study was obtained according to a SUNY Upstate Medical University animal use protocol (Institutional Animal Care and Use Committee nos. 338 and 423). All mice were housed in temperature-controlled rooms on a 12-hour light: 12-hour dark schedule in our animal facility while being fed mouse chow and water *ad libitum*. Animal work was approved by the Institutional Animal Care and Use Committee, and all experimental procedures were carried out in accordance with National Institutes of Health and ARRIVE guidelines on the use of laboratory animals.

The 3-(2,4-dimethoxybenzylidene)-anabaseine (GTS-21), α-bungarotoxin (α-BgTX), and D-(+)-glucose were purchased from Sigma-Aldrich (St. Louis, MO); ELISA kits for mouse GLP-1 were obtained from RayBiotech, Inc. (Norcross, GA). LY294002 (catalog no. 9901) and antibodies against phospho-PI3 kinase p85 (Tyr458)/p55 (Tyr199) [catalog no. 4228; 1:1000 dilution (27)], PI3 kinase p85 (19H8) [catalog no. 4257; 1:1000 dilution (28)], and Akt [catalog no. 9272; 1:1000 dilution (29)] were purchased from Cell Signaling Technology (Danvers, MA). Sodium palmitate (catalog no. sc-215881), Akt1/2 kinase inhibitor (catalog no. sc-300173), rapamycin (catalog no. sc-3504), and antibodies against α7nAChR [H-302; catalog no. sc-5544; 1:200 dilution (30)], GLP-1 [C-17; catalog no. sc-7782; 1:50 dilution (31)], phospho-Akt1/2/3 [Ser 473; catalog no. sc-7985-R; 1:200 dilution (32)], and phospho-p70 S6K α [A-6; catalog no. sc-8416; 1:200 dilution (33)] were purchased from Santa Cruz Biotechnology (Dallas, TX). BAPTA-AM was purchased from Thermo Fisher Scientific (catalog no. B6769; Grand Island, NY). PO_4-AM_3 was purchased from Axxora (catalog no. BLG-P030-003; Farmingdale, NY).

Cell cultures

STC-1 and NCI-H716 cells were purchased from American Type Culture Collection (Manassas, VA). STC-1 cells were cultured in DMEM media (25 mM of glucose) with 10% fetal bovine serum (FBS) and 1% (v/v) penicillin (100 U/mL) and streptomycin (100 μg/mL) (pen-strep). NCI-H716 cells were grown in RPMI 1640 medium with 10% FBS and 1% pen-strep. NCI-H716 cell adhesion was initiated by plating the cells on Matrigel Basement Membrane (catalog no. 354234; BD Biosciences, Bedford, MA) in DMEM supplemented with 10% FBS, 2 mm L-glutamine, and 1% (v/v) pen-strep. GLUTag cells (34) were obtained from Dr. D.J. Drucker (University of Toronto) and cultured in DMEM (5.5 mM of glucose) supplemented with 10% FBS and 1% (v/v) pen-strep. Culture media of GLUTag and STC-1 were exchanged every 3 days, and cells were trypsinized and reseeded when 80% confluence was reached. Newborn mice (C57BL/6) were used for preparation

of mixed primary intestinal cell cultures enriched with L cells as described previously (35).

GLP-1 secretion assay

Two days before each experiment, cells plated in 12-well culture plates coated with Matrigel (BD Biosciences) were allowed to reach 75% to 85% confluence. On the day of the experiment, cells were washed twice with glucose-free Krebs-Ringer medium containing (in mmol/L) 120 NaCl, 5 KCl, 2 $CaCl_2$, 1 $MgCl_2$, 22 $NaHCO_3$, and 0.1 Diprotin A, gassed with 95% O_2/5% CO_2 for 10 minutes, and then supplemented with 0.5% (w/v) BSA. Experiments were performed by incubating the cells in Krebs-Ringer medium containing GTS-21 for 2 hours at 37°C in a tissue culture incubator. For some experiments, cells were pretreated with α-BgTX, LY294002, Akt1/2 kinase inhibitor, rapamycin, BAPTA-AM, and PO_4-AM_3 for 30 minutes in Krebs-Ringer medium before GTS-21 stimulation. At the end of each incubation, media were collected and centrifuged to remove any floating cells. The adherent cells were then lysed using RIPA buffer, and lysates were analyzed for total protein content using the Bradford assay (Bio-Rad Laboratories, Hercules, CA). Bioactive GLP-1 levels in the supernatants were determined by ELISA. Each experiment was repeated three times, and levels of secreted GLP-1 were normalized relative to total protein content expressed as a percentage of levels present in unstimulated control cells. Preliminary studies demonstrated that these signaling inhibitors (LY294002, Akt1/2 inhibitor, and rapamycin) did not alter GLP-1 secretion under the experimental conditions described here.

Cell viability assay

Cell viability was determined using the 3-[4,5-dimethylthiazol-2-yl]-2,5 diphenyl tetrazolium bromide (MTT; catalog no. 298-936-1; Thermo Fisher Scientific) colorimetric assay. Initially, cells were seeded in 96-well plates (10,000 cells per well) so that the indicated test compounds could be evaluated in triplicate assays while maintained in a tissue culture incubator. After the indicated treatment period was reached, 100 μL of 0.5 mg/mL MTT was added to each well. Cells were then incubated for an additional 4 hours at 37°C in a tissue culture incubator. MTT absorbance was then measured at 570 nm by a plate reader (Multiskan Ascents 354; Thermo LabSystems, Grand Island, NY).

Induction of glucotoxicity

Glucotoxicity was induced by exposure of cells to 25.6 mM (for GLP-1 secretion) or 30.6 mM (for cell viability) of glucose for 72 hours. Every 24 hours, the cell culture media were refreshed. For GLP-1 secretion experiments, cells were then washed and treated with GTS-21 for 2 hours in Krebs-Ringer medium after induction of glucotoxicity. In some experiments, cells were incubated with α-BgTX for 30 minutes before GTS-21 stimulation. For cell viability assays after induction of glucotoxicity, cells were washed with 5.6 mM of glucose culture medium ± GTS-21 for 24 hours. To control for osmotic effects of high glucose, equimolar concentrations of mannitol were used.

RT-PCR assay

Total RNA was isolated from cells using the TRIzol method (Gibco Brl; Life Technologies). Total RNA (2 μg) was converted to cDNA using an iScript cDNA Synthesis Kit (Bio-Rad Laboratories) and a thermal cycler. Reverse transcription–negative samples were used to confirm the absence of genomic DNA. PCR was performed with the Step One Plus Real-Time PCR System (Applied Biosystems, Foster City, CA). The primers for mouse α7nAChR were 5′-ATCTGGGCATTGC-CAGTATC-3′ (forward) and 5′-TCCCATGAGATCCCATT-CTC-3′ (reverse; predicted 199-bp product). The primers for human α7nAChR were 5′-CCCGGCAAGAGGAGTGAAA-GGT-3′ (forward) and 5′-TGCAGATGATGGTGAAGACC-3′ (reverse; predicted 843-bp product). A sample containing all reaction reagents except cDNA was used as the RT-PCR negative control in each experiment. Amplified PCR products were visualized on 2% agarose gels to determine product sizes and the specificity of amplification.

Cytosolic Ca^{2+} and cAMP assays

Cells were virally transduced to express the genetically encoded biosensor YC3.6 (36) for cytosolic Ca^{2+} measurements or H188 for cytosolic cAMP measurements (37). Measurements were performed 2 days after transduction in assays of fluorescence resonance energy transfer. Dynamic changes of $[Ca^{2+}]_i$ or $[cAMP]_i$ were monitored in real time by imaging single cells plated on glass coverslips 1 day before each assay. For all assays, tissue culture medium was removed and replaced with a standard extracellular solution containing (in mM) 138 NaCl, 5.6 KCl, 2.6 $CaCl_2$, 1.2 $MgCl_2$, and 10 HEPES (adjusted to pH 7.4 with NaOH) and supplemented with 5.6 mM of glucose. Cells on glass coverslips were then transferred to a temperature-controlled imaging chamber (QE-1; Warner Instruments, Hamden, CT) mounted on a Nikon Ti microscope while maintained at 37°C. Test solutions delivered to the chamber were prewarmed using an in-line heater (SH-27B; Warner Instruments), and the chamber contents were constantly perfused through the chamber at a rate of 2 mL/min using a peristaltic pump (RP-1; Rainin Dynamax, Oakland, CA). MetaFluor software (Molecular Devices, San Jose, CA) was used to control excitation light from a PTI (London, ON, Canada) DeltaRam monochromator, and images were acquired through a Dual-View beamsplitter (MAG Biosystems, BioVision Technologies, Exton, PA) using a Cascade 512B camera (Photometrics, Tuscon, AZ). Fluorescence resonance energy transfer–based measurements for both biosensors were obtained when using excitation light at 440 nm while monitoring the emission light measured simultaneously at 485 and 535 nm. An oil-immersion Nikon 60× objective was used to acquire these images. Data were exported from MetaFluor into Origin 15 software (OriginLab, Northampton, MA) for further processing, plotting, and statistical analysis.

Western blot assays

Cells were lysed on ice using protein lysis buffer containing a protease inhibitor cocktail (Roche, Indianapolis, IN). Samples were then centrifuged at 12,000 rpm at 4°C for 5 minutes. Equal amounts of protein were resolved by SDS-PAGE and transferred onto polyvinylidene difluoride membranes. After blocking with 5% nonfat milk, membranes were probed with the primary and secondary antibodies listed above so that enhanced chemiluminescence-based detection of these proteins could be achieved. Detection of β-actin was used as a loading control.

Immunocytochemistry

Cells were grown in 96-well plates coated with Matrigel. The medium was removed, and cells were rinsed with PBS and fixed in

paraformaldehyde solution for 5 minutes. Intestinal tissue immediately proximal and distal to the appendix was extracted after euthanization, carefully cleaned of fat, fixed, and embedded in paraffin. These paraffin sections were deparaffinized in xylene and then hydrated in serial alcohol solutions. Fixed cells and tissue sections were incubated with 5% normal donkey serum for 1 hour. Cell and tissue sections were then incubated overnight at 4°C with the primary antibodies for GLP-1 [goat polyclonal antibody; catalog no. sc-7985-R; 1:50 dilution; Santa Cruz Biotechnology (32)] and the α7nAChR [rabbit polyclonal antibody; catalog no. sc-5544; 1:50 dilution; Santa Cruz Biotechnology (30)]. After three rinses with PBS, cells and sections were incubated 1 hour at room temperature with the indicated secondary antibodies comprising an Alexa Fluor 488–conjugated donkey anti-rabbit IgG (1:200 dilution; Abcam) or an Alexa Fluor 594–conjugated donkey anti-goat IgG (1:200 dilution; Thermo Fisher Scientific). Cells and sections were then gently rinsed three times with PBS. Finally, Fluoroshield mounting medium was applied, after which samples were imaged by fluorescence immunocytochemistry using a Nikon Eclipse TE2000-U microscope equipped with a Nikon CCD camera.

Small interfering RNA transfection assays

α7nAChR or nontargeting (scrambled) small interfering RNA (siRNA) was delivered by transfection of GLUTag or STC-1 cells using a transfection reagent, as described in the manufacturer's protocol (Santa Cruz Biotechnology). Forty-eight hours after transfection, expression levels of α7nAChR mRNA and protein were measured to determine the α7nAChR knockdown efficiency. Fluorescein-conjugated control siRNA was used to monitor transfection efficiency by fluorescence microscopy. Transfected cells were washed and treated ± GTS-21 (75 μM) for 2 hours, and media were collected to monitor GLP-1 secretion.

Effects of GTS-21 on circulating levels of GLP-1

To monitor effects of GTS-21 on GLP-1 secretion *in vivo*, C57BL/6 mice were administered GTS-21 by intraperitoneal injection at doses of 2, 4, and 8 mg/kg. Serum levels of GLP-1 at the indicated time points after injection were determined by ELISA using the kit described above.

Statistical analysis

Statistical analyses were performed using SPSS software (SPSS Inc., Chicago, IL). Continuous variables were first tested for normality and equality of variances. The results are expressed as the means ± SEM or shown as box and whisker plots from experiments run in triplicate, with the number of independent experiments indicated in the figure legends. Box and whisker plots show mean (solid square), 25% to 75% range (open box), median (line across open box), and minimum and maximum values (whiskers). One-way ANOVA with the *post hoc* Bonferroni test was used in multiple comparisons. Significance is indicated at $P < 0.05$.

Results

α7nAChR expression in L-cell lines and murine intestine

Expression of α7nAChR mRNA in the enteroendocrine L-cell lines GLUTag, STC-1, and NCI-H716 was determined by RT-PCR. As shown in Fig. 1A, PCR products

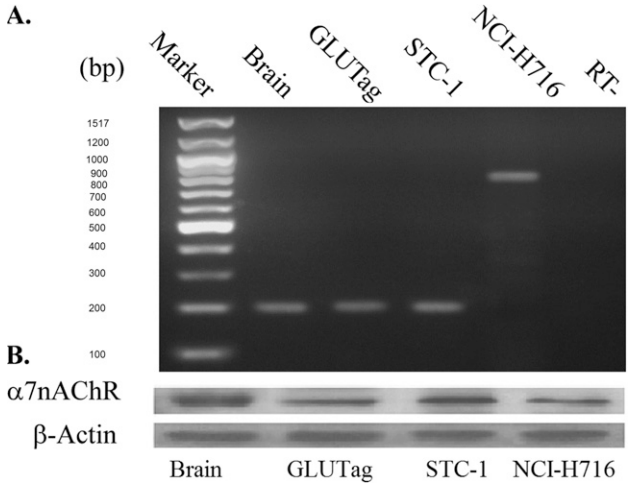

Figure 1. α7nAChR expression in intestinal L cells. (A) α7nAChR mRNA expression was analyzed by RT-PCR. A 199-bp band corresponding to mouse α7nAChR was specifically amplified in mouse brain tissue (positive control), GLUTag cells, and STC-1 cells. An 843-bp band corresponding to human α7nAChR was amplified in NCI-H716 cells. No contamination of genomic DNA was detected in the lane labeled "RT−," which corresponds to PCR reactions run in the absence of reverse transcription. (B) α7nAChR protein expression was detected in mouse brain (positive control), GLUTag, STC-1, and NCI-H716 cells, as evaluated by Western blot analysis (20 μg of protein loaded per lane) using anti-α7nAChR antisera. RT−, reverse transcription–negative.

of the predicted molecular sizes for the α7nAChR (199 bp for murine cells and 843 bp for human cells) were obtained using all L-cell lines. As a positive control, we used mRNA from mouse brain, which is known to express a high level of α7nAChR. Expression of α7nAChR protein in L cells was

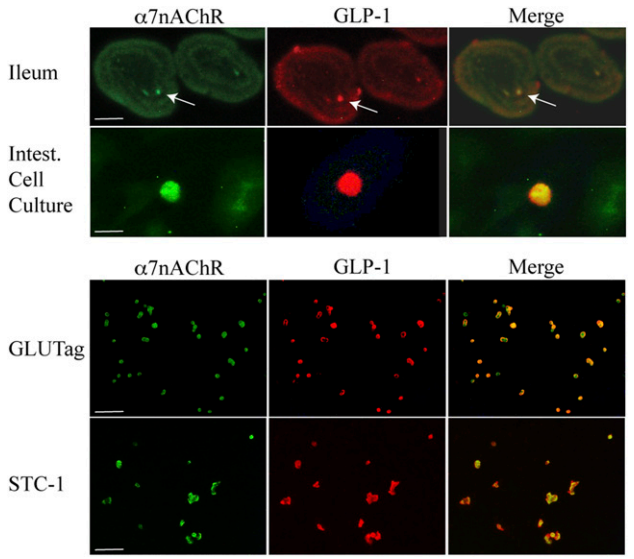

Figure 2. Immunofluorescent staining of α7nAChR and GLP-1. Top two panels show α7nAChR (green) and GLP-1 (red) immunoreactivity in sections of mouse ileum and in primary intestinal (Intest.) cell cultures that contain L-cells (arrows). Merged overlays demonstrate codetection of both immunoreactivities in single L cells (yellow). Bottom two panels show the same as for top panels except that findings are for GLUTag and STC-1 cells. Calibration bars, 100 μm for ileum, GLUTag, and STC-1 or 10 μm for primary intestinal cell cultures.

also evaluated by Western blot analysis. A clear band with a molecular weight of approximately 55 kD was detected in GLUTag, STC-1, and NCI-H716 cell lysates (Fig. 1B). α7nAChR protein from mouse brain was again used as a positive control (Fig. 1B). Next, immunofluorescence microscopy was performed to image α7nAChR expression in primary mouse small intestinal cell cultures, sections of mouse ileum, and GLUTag or STC-1 cells that were double-stained for GLP-1 and α7nAChR. Cells demonstrated immune-positive staining for GLP-1 (red) and α7nAChR (green), and merged images validated their colocalization (Fig. 2). Similar findings were obtained with NCI-H716 cells (data not shown). L cells, identified by GLP-1 staining, are sparse in the primary intestinal epithelial cell cultures and intestinal villi. However, most cells staining positive for GLP-1 also expressed α7nAChR (Fig. 2).

α7nAChR-regulated GLP-1 secretion

The role of α7nAChR in the regulation of GLP-1 secretion was evaluated using GLUTag, STC-1, and NCI-H716 cell lines, as well as mixed intestinal mouse primary epithelial cell cultures treated for 2 hours with or without GTS-21. For comparison, basal GLP-1 secretion was measured in glucose-free Krebs-Ringer medium in 12-well plates for each cell type. Basal [GLP-1] was 30.5 ± 2.1 pg/mL in GLUTag (n = 18), 25.6 ± 3.9 pg/mL in STC-1 (n = 18), 40.1 ± 3.2 pg/mL in NCI-H716 (n = 19), and 14.8 ± 2.7 pg/mL in intestinal epithelial cell cultures (n = 12).

The dose-dependent action of GTS-21 in assays of GLP-1 secretion is shown in Fig. 3A. GTS-21 significantly increased GLP-1 secretion, indicating a functional role for α7nAChR in L cells. To confirm that GTS-21–induced GLP-1 secretion was a result of α7nAChR activation, GLUTag, STC-1, NCI-H716, and mixed primary intestinal epithelial cell cultures were preincubated with the α7nAChR antagonist α-BgTX (100 nM) before GTS-21 stimulation. For all cell types tested, the GTS-21–stimulated GLP-1 secretion was abrogated after α-BgTX pretreatment (Fig. 3B). Next, we examined whether siRNA knockdown of α7nAChR inhibited GTS-21–stimulated GLP-1 secretion. First, we confirmed that

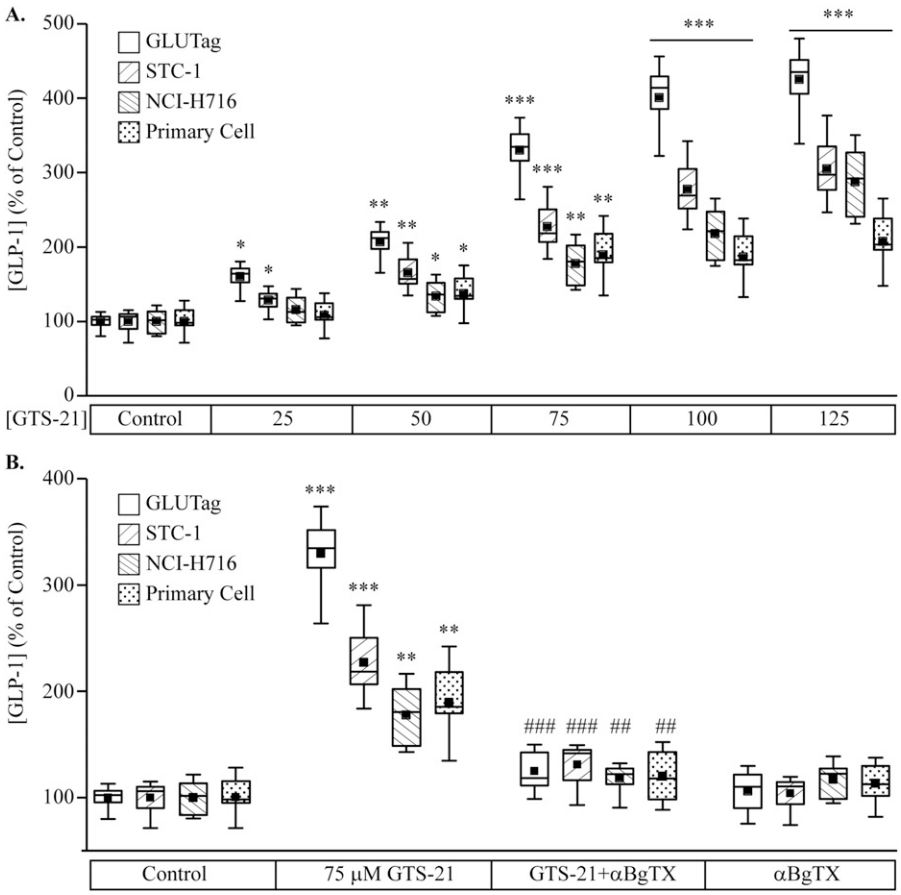

Figure 3. Effects of GTS-21 and α-bungarotoxin (α-BgTX) on GLP-1 secretion. (A) GLUTag, STC-1, NCI-H716, and mouse primary intestinal cell cultures were treated with PBS (control) or increasing concentrations of GTS-21 for 2 h. Secreted GLP-1 was measured using ELISA assays and is expressed as the percentage change relative to control for each cell type. $^{*}P < 0.05$, $^{**}P < 0.01$, $^{***}P < 0.001$ *vs.* control group (n = 8 to 10). (B) GLUTag, STC-1, NCI-H716, and mouse primary intestinal cell cultures were preincubated with 100 nM of α-BgTX for 30 min before 2-h stimulation with GTS-21. $^{**}P < 0.01$, $^{***}P < 0.001$ *vs.* control group; $^{\#\#}P < 0.01$, $^{\#\#\#}P < 0.001$ *vs.* GTS-21 group (n = 8 to 10). Box and whisker plots show the mean (solid box), 25% to 75% range (open box), median (horizontal line within open box), and minimum and maximum values (whiskers).

treatment with α7nACHR siRNA resulted in decreased expression of α7nAChR mRNA (Fig. 4A) and protein (Fig. 4B) in GLUTag and STC-1 cells. We also demonstrated that knockdown of α7nAChR attenuated the ability of GTS-21 to stimulate GLP-1 release in GLUTag and STC-1 cells (Fig. 4C and 4D, respectively).

GTS-21 counteracted L-cell glucotoxicity

Impaired GLP-1 secretion in T2DM appears to be caused in part by the effects of chronic hyperglycemia, which generates glucotoxicity. Here, GLUTag cells were exposed to 25.6 mM of glucose for 72 hours to induce glucotoxicity so a potential restorative effect of GTS-21 on GLP-1 secretion could be examined. Glucotoxic cell culture conditions decrease basal GLP-1 secretion in GLUTag cells, and this inhibition was reversed by treatment with GTS-21 (Fig. 5A). As expected, pretreatment of GLUTag cells with α-BgTX counteracted this secretagogue action of GTS-21. These data provide an indication that α7nAChR activation

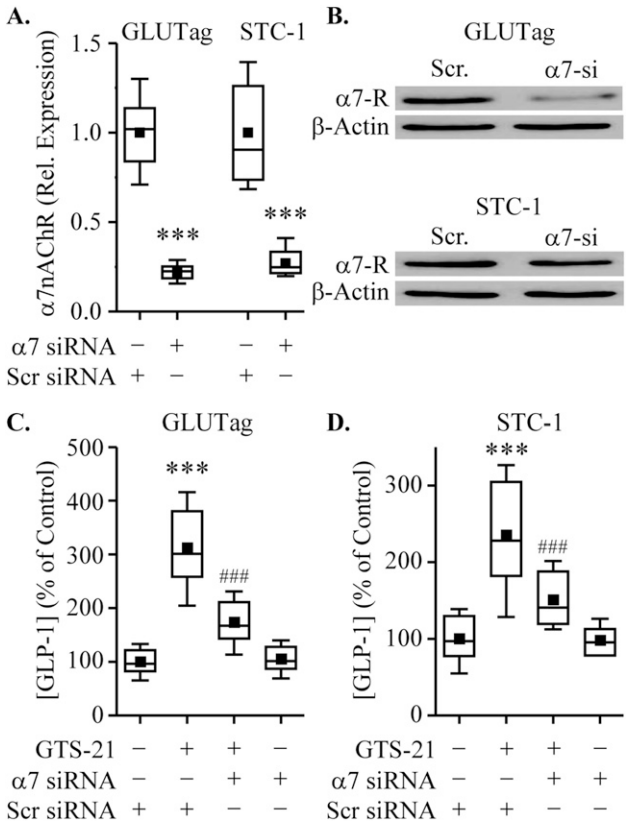

Figure 4. α7nAChR siRNA regulates α7nAChR expression and GLP-1 secretion. (A and B) Cells were transfected with (+) or without (−) α7nAChR (α7-si) or nontargeting [scrambled (Scr)] siRNA for 48 h. Levels of α7nAChR (A) mRNA and (B) protein (α7-R) were measured by RT-PCR and Western blot analysis. Cells transfected with α7nAChR or Scr siRNA (48 h) were treated with GTS-21 (75μM) for 2 h, and GLP-1 secretion was determined. (C and D) Knockdown of α7nAChR reduced GLP-1 secretion induced by GTS-21 in (C) GLUTag and (D) STC-1 cells. $^{***}P < 0.001$ *vs.* scrambled siRNA group; $^{###}P < 0.001$ *vs.* scrambled siRNA plus GTS-21 group (n = 7 to 8).

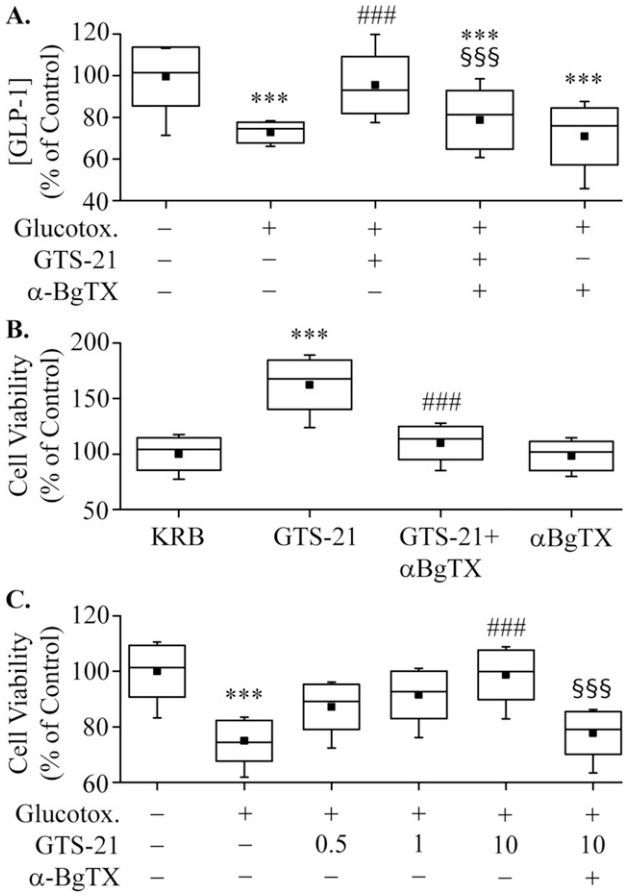

Figure 5. Effects of glucotoxicity (Glucotox.). (A) GLUTag cells were incubated for 72 h in either 5.6 mM (control) or 25.6 mM of glucose, washed and pretreated ± α-BgTX for 30 min, then stimulated with PBS or GTS-21 (75 μM) for 2 h. The amount of GLP-1 released into the medium was measured by ELISA. $^{***}P < 0.001$ *vs.* control group; $^{###}P < 0.001$ *vs.* PBS group; $^{§§§}P < 0.001$ *vs.* GTS-21 group (n = 7). (B) GLUTag cells were preincubated with 100 nM of α-BgTX for 30 min and then were treated with PBS or GTS-21 (1 μM) for 24 h. Cell viability was determined by the MTT assay. $^{***}P < 0.001$ *vs.* PBS group; $^{###}P < 0.001$ *vs.* GTS-21 group (n = 8). (C) GLUTag cells were treated with 5.6 mM (control) or 30.6 mM (Glucotox.) of glucose for 72 h. GLUTag cells were then stimulated with GTS-21 (1 μM) for 24 h with (+) or without (−) preincubation using α-BgTX (100 nM). Cell viability was then measured by MTT assay. $^{***}P < 0.001$ *vs.* control group; $^{###}P < 0.001$ *vs.* PBS group; $^{§§§}P < 0.001$ *vs.* 10-μM GTS-21 alone group (n = 7).

restores GLP-1 secretion to normal levels under conditions of glucotoxicity.

Chronic elevation of glucose or lipid levels may also affect L-cell viability in addition to effects on GLP-1 secretion. We therefore examined the effects of GTS-21 on L-cell viability using the MTT assay and GLUTag cells cultured in media that contained either normal or elevated concentrations of glucose. Under normoglycemic conditions, treatment with GTS-21 for 24 hours enhanced the number and viability of GLUTag cells (Fig. 5B). Treatment with α-BgTX (100 nM) alone had no effect on cell viability but fully abrogated the effects of GTS-21 on cell viability and number. Several lines of evidence suggest that

increasing the number of intestinal L cells might represent a promising mechanism for augmenting GLP-1 secretion and improving glycemic control (18).

To further characterize the effects of GTS-21 on L-cell viability, we examined its effects under glucotoxic culture conditions (16, 17). In these experiments, GLUTag cells were exposed to 30.6 mM of glucose for 72 hours, resulting in decreased cell viability (Fig. 5C). Increasing concentrations of GTS-21 ameliorated the deleterious effects of glucotoxicity on cell viability, and α-BgTX blocked this effect, thereby establishing that L-cell viability is under the control of α7nAChR.

GTS-21 increased $[Ca^{2+}]_i$ but not $[cAMP]_i$

α7nAChR has ionotropic effects by forming a Ca^{2+}-permeant cation channel (38), and it also exerts metabotropic effects through G protein signaling (39). These properties lead to the prediction that GTS-21 may stimulate GLP-1 secretion through elevation of $[Ca^{2+}]_i$. When GLUTag cells expressing the $[Ca^{2+}]_i$ reporter YC3.6 were stimulated with GTS-21, an oscillatory rise of $[Ca^{2+}]_i$ was observed (Fig. 6A and 6B). Although GLP-1 secretion has also been stimulated by cAMP (40), GTS-21 had no effect on $[cAMP]_i$ in GLUTag cells (Fig. 6C). Thus, Ca^{2+} but not cAMP mediates the action of GTS-21 to stimulate GLP-1 release.

PI3K/AKT/mTOR signaling was stimulated by GTS-21

The PI3K/Akt/mTOR signaling pathway is reported to be activated by α7nAChR agonists, and it is involved in the regulation of cell proliferation, survival, and metabolism. We found a significant increase in the levels of phosphorylated PI3K, Akt, and p70 S6K 2 hours after treatment of GLUTag cells with GTS-21 (Fig. 7A). As predicted, pretreatment with α-BgTX reduced these actions of GTS-21 (Fig. 7A), as was also the case for a PI3K inhibitor (LY294002), an Akt1/2 kinase inhibitor, and an mTOR inhibitor (rapamycin) (Fig. 7B). However, none of these inhibitors of growth factor signaling pathways reduced GLP-1 secretion in response to GTS-21 (data not shown). In contrast, loading of cells with the membrane-permeable Ca^{2+} chelator prodrug BAPTA-AM reduced GLP-1 secretion in response to GTS-21, whereas the negative control PO_4-AM_3 that fails to buffer Ca^{2+} was ineffective (Fig. 7C). Surprisingly, activation of the PI3K/Akt/p70 S6K pathway by GTS-21 was reduced in BAPTA-AM–loaded cells but not in PO_4-AM_3–loaded cells (Fig. 7C). Thus Ca^{2+} serves as a permissive factor—or possibly a direct coupling factor—for GTS-21–stimulated growth factor signaling.

Effects of GTS-21 on circulating GLP-1

Finally, we tested whether GTS-21 stimulated GLP-1 secretion *in vivo* in C57BL/6 mice. Mice were injected intraperitoneally with 2, 4, and 8 mg/kg of GTS-21, and the circulating levels of GLP-1 were measured 1 hour later. As shown in Fig. 8A, there was a 34% increase in circulating levels of GLP-1 after administration of 2 mg/kg of GTS-21 and a 93% increase after administration of 4 mg/kg of GTS-21. Increasing the GTS-21 dose to 8 mg/kg had no additional significant effect. As shown in Fig. 8B, the increase in circulating GLP-1 level after administration of 4 mg/kg of GTS-21 was maintained for 4 hours.

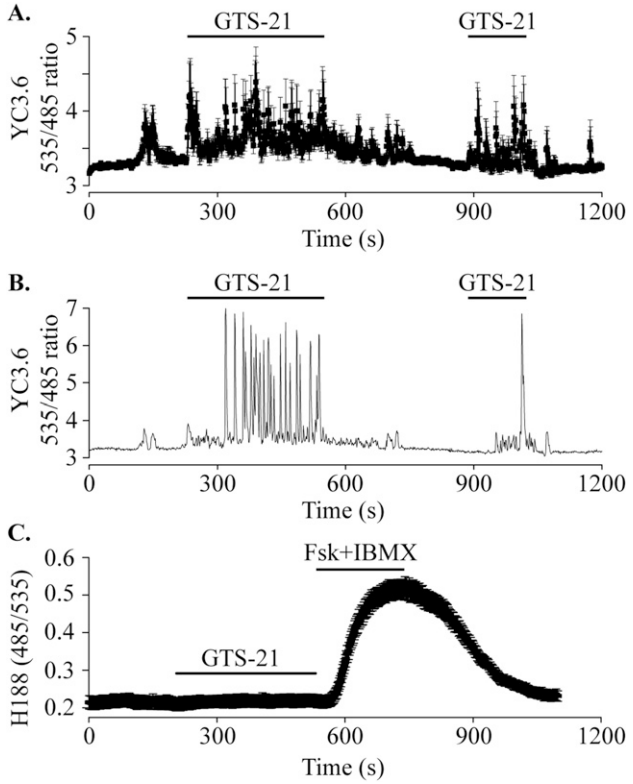

Figure 6. Assays for cytosolic Ca^{2+} and cAMP. (A) GLUTag cells transduced with the Ca^{2+} reporter YC3.6 were perifused with 5.6 mM of glucose standard extracellular solution at 37°C. GTS-21 (100 μM) was applied (indicated by bars) and induced an oscillatory rise of $[Ca^{2+}]_i$. Data are plotted as mean ± SEM for 9 cells from a single experiment and are representative of 64 cells from three independent transductions. (B) Single cell $[Ca^{2+}]_i$ response to GTS-21 (100 μM) taken from the record shown in (A). The single-cell record highlights the oscillatory $[Ca^{2+}]_i$ response. (C) GLUTag cells transduced with the cAMP reporter H188 were perifused with GTS-21 (100 μM) followed by forskolin (Fsk; 5 μM) + 3-isobutyl-1-methylxanthine (IBMX; 100 μM). GTS-21 had no effect on $[cAMP]_i$, whereas the positive control (Fsk + IBMX) reversibly elevated [cAMP]. Data are plotted as mean ± SEM for 24 cells from three experiments and are representative of 62 cells from three independent viral transductions.

Discussion

Findings reported here demonstrated expression of α7nAChR in L-cell lines that secrete GLP-1 and also in GLP-1–positive L cells of the mouse intestine. Expression of α7nAChR in human L cells has yet to be elaborated.

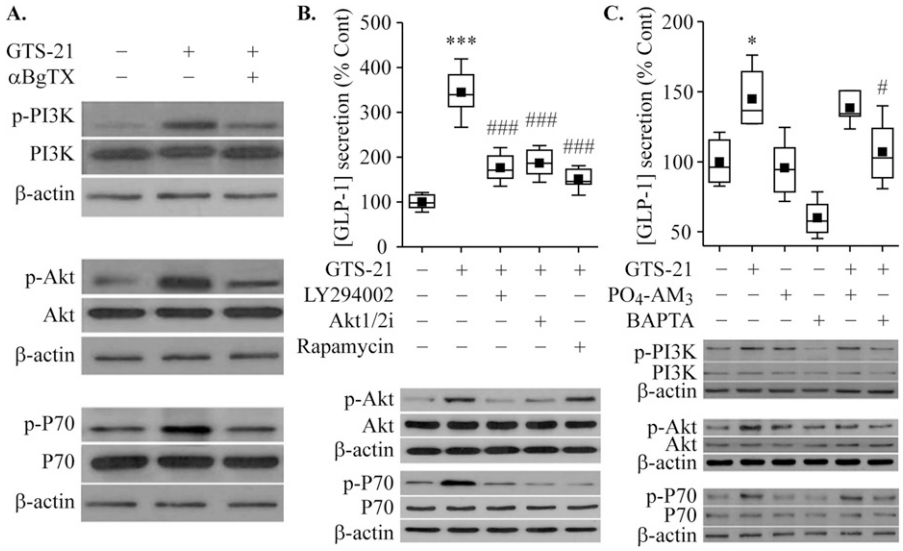

Figure 7. Regulation of GLP-1 secretion by the PI3K/AKT/mTOR signaling pathway. (A–C) Stimulation of α7nAChR by GTS-21 enhanced GLP-1 secretion through PI3K/AKT/mTOR activation in GLUTag cells. (A) PI3K/AKT/mTOR activation. Cells were pretreated with α-BgTX (100 nM) for 30 min, then treated with GTS-21 (75 μM) for 2 h. The cell lysate was subjected to Western blotting. (B) Effects of GTS-21 on GLP-1 secretion were abrogated by the inhibitor of the PI3K/AKT/mTOR signaling pathway. Cells were pretreated with LY294002 (10 μM), Akt1/2 kinase inhibitor (5 μM), and rapamycin (2 nM) for 30 min, then treated with GTS-21 (75 μM) for 2 h. The amount of GLP-1 released into the medium was measured, and the cell lysate was subjected to Western blot analysis. (C) Effect of BAPTA-AM on GLP-1 secretion. Cells were pretreated with BAPTA-AM (10 μM) or PO_4-AM_3 (3.3 μM) for 30 min, then treated with GTS-21 (75 μM) for 2 h. Cell lysates were subjected to Western blotting. $^{*}P < 0.05$, $^{***}P < 0.001$ *vs.* control group; $^{\#}P < 0.05$, $^{\#\#\#}P < 0.001$ *vs.* GTS-21 group (n = 5 to 8).

Activation of α7nAChR increased GLP-1 secretion and enhanced L-cell viability in the presence or absence of glucotoxicity. Just as important, mice treated with GTS-21 showed an increase in circulating GLP-1 level in time- and dose-dependent manners. α7nAChR activation by GTS-21 induced GLP-1 release and enhanced L-cell viability, and these effects resulted from a stimulation of the Ca^{2+} and PI3K/Akt/mTOR signaling pathways. A schematic model of the α7nAChR signaling pathway that we elucidated for L cells is shown in Fig. 9. Interestingly, nicotine stimulates smooth muscle cell proliferation through α7nAChR-mediated activation of PI3K/Akt signaling (45), and the PI3K/Akt/mTOR pathway is involved in vascular endothelial growth factor secretion from STC-1 cells (46), thereby suggesting conserved mechanisms of α7nAChR growth factor–like signaling across different cell types.

Prior studies showed that GLP-1 secretion from L cells was maintained by vagal tone (10), but a potential role for α7nAChR was not documented. However, enteroendocrine cells can coexpress and release GLP-1, PYY, and neurotensin (47), and vagal neurons innervating the small intestine of mice have been reported (48). Potentially, vagal release of acetylcholine stimulates GLP-1 secretion through activation of the L-cell α7nAChR.

GLP-1 is conventionally viewed as a potent incretin hormone, and GLP-1 analogs or dipeptidyl peptidase-4 inhibitors are now used for the treatment of T2DM (5, 6). Although no GLP-1–releasing agent has been approved for use in humans with T2DM, this is an area of continued interest within the drug discovery community (7). In our *in vitro* studies of L cells reported here, α7nAChR activation by the selective agonist GTS-21 promoted GLP-1 secretion under normoglycemic conditions and also under conditions of glucotoxicity. Consistent with our data, a correlation between α7nAChR activity and improved glucose homeostasis was reported previously (49, 50). Because α7nAChR agonists such as GTS-21 have shown safety and efficacy in clinical trials of nervous system diseases, they might constitute a novel strategy to achieve neuroprotective effects (21). Extending on this idea, α7nAChR agonists may therefore be promising GLP-1–releasing agents for improving glucose homeostasis in T2DM. GLP-1R mRNA was previously identified in multiple organ systems, and beneficial extrapancreatic effects of GLP-1 exist (51, 52). Therefore, by promoting GLP-1 secretion and activation of the GLP-1 receptor, α7nAChR agonists not only may indirectly promote insulin secretion but also may have beneficial effects in other tissues.

Reduced levels of plasma GLP-1 in patients with T2DM have been reported as well as reduced numbers of GLP-1–producing intestinal cells, and these alterations are positively correlated to obesity and insulin resistance (53). Here, we report that α7nAChR stimulation for 24 hours promoted GLUTag cell viability. Moreover, the viability of GLUTag cells improved with α7nAChR stimulation in the presence of glucotoxicity. Because

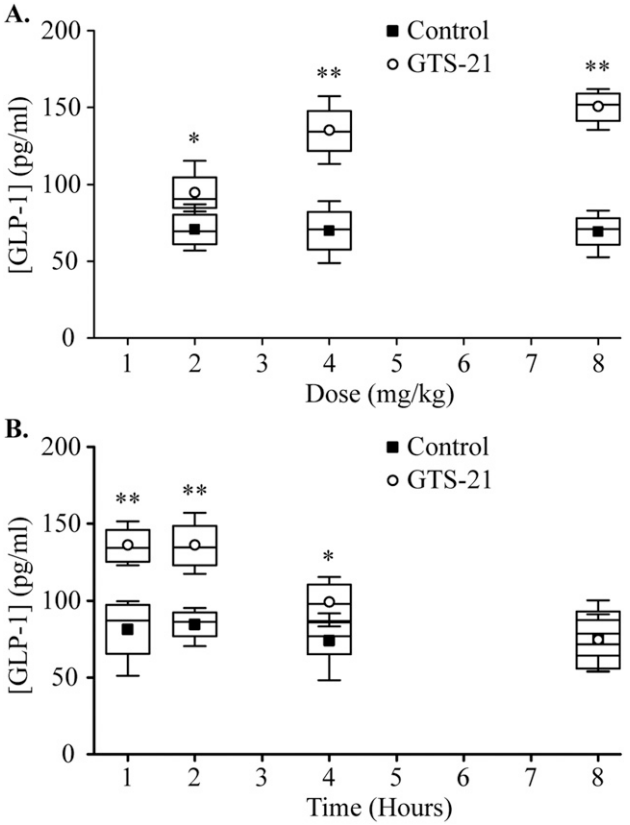

Figure 8. Effects of GTS-21 on circulating GLP-1. (A) Mice were injected intraperitoneally with 2 to 8 mg/kg of GTS-21 or normal saline (vehicle). Blood samples were collected 1 h later, and GLP-1 levels were measured by ELISA. $*P < 0.05$, $**P < 0.01$ *vs.* control group (n = 4 to 5). (B) Mice were injected with 4 mg/kg of GTS-21, and circulating GLP-1 was measured at 1, 2, 4, and 8 h later by ELISA. $*P < 0.05$, $**P < 0.01$ *vs.* control group (n = 4 or 5).

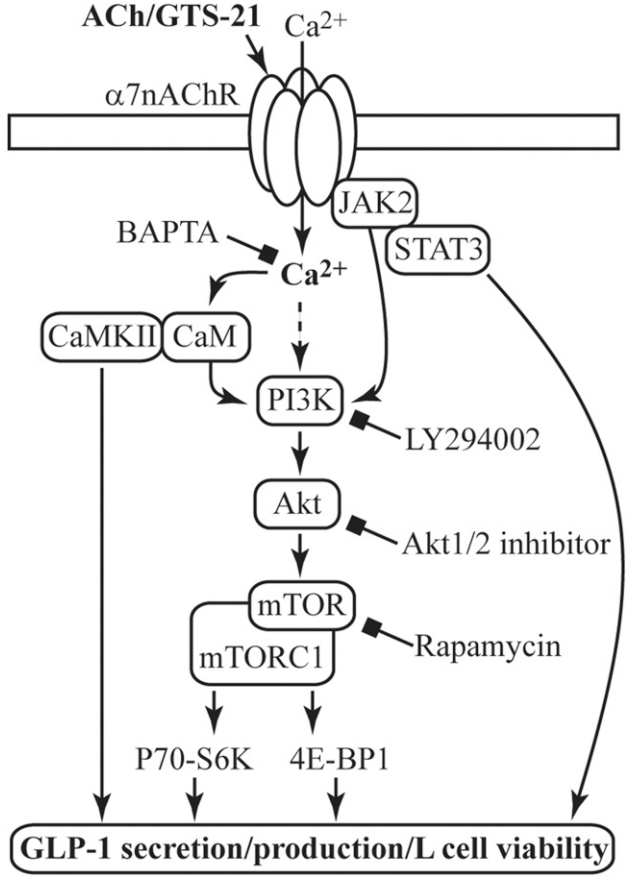

Figure 9. A model for α7nAChR coupling to L-cell function, growth, and survival. Acetylcholine (ACh) or GTS-21 activates α7nAChR and promotes Ca^{2+} influx. Activation of the PI3K/Akt/mTOR pathway downstream of α7nAChR is involved in regulating GLP-1 secretion and cell viability, as revealed by the use of LY294002 (PI3K inhibitor), Akt1/2 kinase inhibitor, or rapamycin (mTOR inhibitor). Coupling of α7nAChR to PI3K activation can occur through several pathways including Ca^{2+}-calmodulin (CaM) (41) and Janus kinase 2 (JAK2) (42). Ca^{2+} can also promote GLP-1 secretion directly or through Ca^{2+}/calmodulin–dependent kinase II (CaMKII) (43). The Ca^{2+} chelator BAPTA-AM inhibits all depicted effects of GST-21. Numerous downstream effectors of the metabolically regulated mTOR complex 1 (mTORC1) (44) are involved in cell viability, and determining which pathways are important to L-cell biology requires further investigation.

glucotoxicity induces apoptosis in GLUTag cells (17), we propose that α7nAChR agonists enhance GLUTag cell viability through antiapoptotic effects, similar to their neuroprotective effects (42). Furthermore, we propose that this beneficial effect is explained by a mechanism of convergent Ca^{2+} and PI3K/Akt/mTOR signaling in L cells (Fig. 9). Still, it is important to note that additional signaling mechanisms are potentially under the control of α7nAChR. For example, Janus kinase 2 (JAK2) mediates the neuroprotective (42) and beneficial glycemic effects of α7nAChR agonists (49). And JAK2 is reported to be inhibitory for insulin secretion in rat islets (54).

In contrast to the central hypothesis presented here, in which GTS-21 exerts a direct action to promote L-cell viability (Fig. 9), it is possible that L-cell α7nAChR activation leads to autocrine or paracrine factor release in the intestine, thereby leading to indirect stimulation of L-cell viability (55). Modulation of L-cell number is a potentially novel therapeutic strategy to improve glycemic control (18), thereby suggesting that α7nAChR stimulation might increase L-cell numbers in patients with T2DM. Because studies of other cell types revealed PI3K/Akt activation downstream of α7nAChR (42, 45, 56), a PI3K/Akt/mTOR pathway might mediate a restorative action of GST-21 to improve L-cell viability under conditions of T2DM. Indeed, mTOR activation links energy supply with the production and secretion of GLP-1 in L cells (57). Thus, future preclinical studies will focus on underlying mechanisms by which α7nAChR activation affects L-cell proliferation, apoptosis, and differentiation in animal models of T2DM.

Conclusion

Enteroendocrine L cells express α7nAChR, and activation of α7nAChR enhances GLP-1 secretion, an effect attributable to elevated levels of cytosolic $[Ca^{2+}]_i$.

Moreover, stimulation of α7nAChR enhances L-cell viability under glucotoxic conditions. Ca^{2+} participates as a necessary cofactor to support PI3K/Akt/mTOR activation, whereas acute inhibition of these growth factor signaling pathways fails to alter GLP-1 secretion. Thus, such growth factor signaling pathways appear to be primary determinants of L-cell viability, survival, and cytoprotection. Because we found that GTS-21 elevated circulating levels of GLP-1 *in vivo*, it may be feasible to use selective α7nAChR agonists, or positive allosteric modulators, as GLP-1–releasing agents and/or L-cell trophic factors with potential therapeutic value in T2DM.

Acknowledgments

Financial Support: This work was supported by National Institute of Diabetes and Digestive and Kidney Diseases Grant no. R01 DK069575 (to G.G.H.). R.N.C. acknowledges the support of the Holz Laboratory Diabetes Research Fund of the Health Science Center Foundation of SUNY Upstate Medical University.

Author Contributions: D.W., Q.M., C.A.L., G.G.H., and R.N.C. designed the experiments. D.W. and Q.M. performed cell cultures and RT-PCR. Q.M. performed quantitative RT-PCR, immunocytochemistry, and GLP-1 release assays using intestinal cell cultures. Q.M., N.Y., and L.Z. performed the Western blots. C.A.L. performed the Ca^{2+} and cAMP measurements. D.W., Q.M., and R.N.C. conceived the project. D.W., Q.M., C.A.L, G.G.H., C.W., and R.N.C. wrote and edited the manuscript.

Correspondence: Robert N. Cooney, MD, Department of Surgery, SUNY Upstate Medical University, 750 East Adams Street, Suite 8141, Syracuse, New York 13210. E-mail: cooneyr@upstate.edu; or Chunting Wang, MD, Department of Critical Care Medicine, Shandong Provincial Hospital, Shandong University, 9677 Jing 10 Road, Jinan 250101, Shandong, China. E-mail: wcteicu@126.com.

Disclosure Summary: The authors have nothing to disclose.

References

1. Habib AM, Richards P, Rogers GJ, Reimann F, Gribble FM. Co-localisation and secretion of glucagon-like peptide 1 and peptide YY from primary cultured human L cells. *Diabetologia*. 2013; **56**(6):1413–1416.
2. Vilsbøll T, Holst JJ. Incretins, insulin secretion and type 2 diabetes mellitus. *Diabetologia*. 2004;**47**(3):357–366.
3. Abbott CR, Monteiro M, Small CJ, Sajedi A, Smith KL, Parkinson JR, Ghatei MA, Bloom SR. The inhibitory effects of peripheral administration of peptide YY(3-36) and glucagon-like peptide-1 on food intake are attenuated by ablation of the vagal-brainstem-hypothalamic pathway. *Brain Res*. 2005;**1044**(1):127–131.
4. Krieger JP, Arnold M, Pettersen KG, Lossel P, Langhans W, Lee SJ. Knockdown of GLP-1 receptors in vagal afferents affects normal food intake and glycemia. *Diabetes*. 2016;**65**(1):34–43.
5. Courtney H, Nayar R, Rajeswaran C, Jandhyala R. Long-term management of type 2 diabetes with glucagon-like peptide-1 receptor agonists. *Diabetes Metab Syndr Obes*. 2017;**10**:79–87.
6. Holst JJ, Deacon CF. Glucagon-like peptide-1 mediates the therapeutic actions of DPP-IV inhibitors. *Diabetologia*. 2005;**48**(4): 612–615.
7. Kuhre RE, Holst JJ, Kappe C. The regulation of function, growth and survival of GLP-1-producing L-cells. *Clin Sci (Lond)*. 2016; **130**(2):79–91.
8. Rask E, Olsson T, Söderberg S, Johnson O, Seckl J, Holst JJ, Ahrén B; Northern Sweden Monitoring of Trends and Determinants in Cardiovascular Disease (MONICA). Impaired incretin response after a mixed meal is associated with insulin resistance in non-diabetic men. *Diabetes Care*. 2001;**24**(9):1640–1645.
9. Roberge JN, Brubaker PL. Regulation of intestinal proglucagon-derived peptide secretion by glucose-dependent insulinotropic peptide in a novel enteroendocrine loop. *Endocrinology*. 1993; **133**(1):233–240.
10. Rocca AS, Brubaker PL. Role of the vagus nerve in mediating proximal nutrient-induced glucagon-like peptide-1 secretion. *Endocrinology*. 1999;**140**(4):1687–1694.
11. Plaisancie P, Bernard C, Chayvialle JA, Cuber JC. Regulation of glucagon-like peptide-1-(7-36) amide secretion by intestinal neurotransmitters and hormones in the isolated vascularly perfused rat colon. *Endocrinology*. 1994;**135**(6):2398–2403.
12. Everard A, Lazarevic V, Derrien M, Girard M, Muccioli GG, Neyrinck AM, Possemiers S, Van Holle A, François P, de Vos WM, Delzenne NM, Schrenzel J, Cani PD. Responses of gut microbiota and glucose and lipid metabolism to prebiotics in genetic obese and diet-induced leptin-resistant mice. *Diabetes*. 2011;**60**(11): 2775–2786.
13. Greiner T, Bäckhed F. Effects of the gut microbiota on obesity and glucose homeostasis. *Trends Endocrinol Metab*. 2011;**22**(4):117–123.
14. Kaji I, Karaki S, Tanaka R, Kuwahara A. Density distribution of free fatty acid receptor 2 (FFA2)-expressing and GLP-1-producing enteroendocrine L cells in human and rat lower intestine, and increased cell numbers after ingestion of fructo-oligosaccharide. *J Mol Histol*. 2011;**42**(1):27–38.
15. Kappe C, Zhang Q, Nyström T, Sjöholm A. Effects of high-fat diet and the anti-diabetic drug metformin on circulating GLP-1 and the relative number of intestinal L-cells. *Diabetol Metab Syndr*. 2014; **6**(1):70.
16. Urbano F, Filippello A, Di Pino A, Barbagallo D, Di Mauro S, Pappalardo A, Rabuazzo AM, Purrello M, Purrello F, Piro S. Altered expression of uncoupling protein 2 in GLP-1-producing cells after chronic high glucose exposure: implications for the pathogenesis of diabetes mellitus. *Am J Physiol Cell Physiol*. 2016; **310**(7):C558–C567.
17. Vasu S, Moffett RC, McClenaghan NH, Flatt PR. Differential molecular and cellular responses of GLP-1 secreting L-cells and pancreatic alpha cells to glucotoxicity and lipotoxicity. *Exp Cell Res*. 2015;**336**(1):100–108.
18. Petersen N, Reimann F, Bartfeld S, Farin HF, Ringnalda FC, Vries RG, van den Brink S, Clevers H, Gribble FM, de Koning EJ. Generation of L cells in mouse and human small intestine organoids. *Diabetes*. 2014;**63**(2):410–420.
19. Petersen N, Reimann F, van Es JH, van den Berg BM, Kroone C, Pais R, Jansen E, Clevers H, Gribble FM, de Koning EJ. Targeting development of incretin-producing cells increases insulin secretion. *J Clin Invest*. 2015;**125**(1):379–385.
20. Bouzat C, Lasala M, Nielsen BE, Corradi J, Esandi MDC. Molecular function of α7 nicotinic receptors as drug targets. *J Physiol*. 2018;**596**(10):1847–1861.
21. Bertrand D, Lee CH, Flood D, Marger F, Donnelly-Roberts D. Therapeutic potential of α7 nicotinic acetylcholine receptors. *Pharmacol Rev*. 2015;**67**(4):1025–1073.
22. Anini Y, Brubaker PL. Muscarinic receptors control glucagon-like peptide 1 secretion by human endocrine L cells. *Endocrinology*. 2003;**144**(7):3244–3250.
23. Qian J, Mummalaneni SK, Alkahtani RM, Mahavadi S, Murthy KS, Grider JR, Lyall V. Nicotine-induced effects on nicotinic

acetylcholine receptors (nAChRs), Ca^{2+} and brain-derived neurotrophic factor (BDNF) in STC-1 cells. *PLoS One*. 2016;**11**(11):e0166565.
24. Kuhre RE, Wewer Albrechtsen NJ, Deacon CF, Balk-Møller E, Rehfeld JF, Reimann F, Gribble FM, Holst JJ. Peptide production and secretion in GLUTag, NCI-H716, and STC-1 cells: a comparison to native L-cells. *J Mol Endocrinol*. 2016;**56**(3):201–211.
25. Brubaker PL, Schloos J, Drucker DJ. Regulation of glucagon-like peptide-1 synthesis and secretion in the GLUTag enteroendocrine cell line. *Endocrinology*. 1998;**139**(10):4108–4114.
26. Drucker DJ, Jin T, Asa SL, Young TA, Brubaker PL. Activation of proglucagon gene transcription by protein kinase-A in a novel mouse enteroendocrine cell line. *Mol Endocrinol*. 1994;**8**(12):1646–1655.
27. RRID:AB_659940.
28. RRID:AB_659889.
29. RRID:AB_329827.
30. RRID:AB_2229517.
31. RRID:AB_2107325.
32. RRID:AB_667741.
33. RRID:AB_2182257.
34. RRID:CVCL_J406.
35. Reimann F, Habib AM, Tolhurst G, Parker HE, Rogers GJ, Gribble FM. Glucose sensing in L cells: a primary cell study. *Cell Metab*. 2008;**8**(6):532–539.
36. Nagai T, Yamada S, Tominaga T, Ichikawa M, Miyawaki A. Expanded dynamic range of fluorescent indicators for $Ca^{(2+)}$ by circularly permuted yellow fluorescent proteins. *Proc Natl Acad Sci USA*. 2004;**101**(29):10554–10559.
37. Klarenbeek J, Goedhart J, van Batenburg A, Groenewald D, Jalink K. Fourth-generation epac-based FRET sensors for cAMP feature exceptional brightness, photostability and dynamic range: characterization of dedicated sensors for FLIM, for ratiometry and with high affinity. *PLoS One*. 2015;**10**(4):e0122513.
38. Corradi J, Bouzat C. Understanding the bases of function and modulation of α7 nicotinic receptors: implications for drug discovery. *Mol Pharmacol*. 2016;**90**(3):288–299.
39. King JR, Nordman JC, Bridges SP, Lin MK, Kabbani N. Identification and characterization of a G protein-binding cluster in α7 nicotinic acetylcholine receptors. *J Biol Chem*. 2015;**290**(33):20060–20070.
40. Tian L, Jin T. The incretin hormone GLP-1 and mechanisms underlying its secretion. *J Diabetes*. 2016;**8**(6):753–765.
41. Zhang M, Jang H, Gaponenko V, Nussinov R. Phosphorylated calmodulin promotes PI3K activation by binding to the SH_2 domains. *Biophys J*. 2017;**113**(9):1956–1967.
42. Shaw S, Bencherif M, Marrero MB. Janus kinase 2, an early target of α7 nicotinic acetylcholine receptor-mediated neuroprotection against Abeta-(1-42) amyloid. *J Biol Chem*. 2002;**277**(47):44920–44924.
43. Kato M, Tani T, Terahara N, Tsuda T. The anthocyanin delphinidin 3-rutinoside stimulates glucagon-like peptide-1 secretion in murine GLUTag cell line via the Ca^{2+}/calmodulin-dependent kinase II pathway. *PLoS One*. 2015;**10**(5):e0126157.
44. Ben-Sahra I, Manning BD. mTORC1 signaling and the metabolic control of cell growth. *Curr Opin Cell Biol*. 2017;**45**:72–82.
45. Hong W, Peng G, Hao B, Liao B, Zhao Z, Zhou Y, Peng F, Ye X, Huang L, Zheng M, Pu J, Liang C, Yi E, Peng H, Li B, Ran P. Nicotine-induced airway smooth muscle cell proliferation involves TRPC6-dependent calcium influx via α7 nAChR. *Cell Physiol Biochem*. 2017;**43**(3):986–1002.
46. Villaume K, Blanc M, Gouysse G, Walter T, Couderc C, Nejjari M, Vercherat C, Cordier-Bussat M, Roche C, Scoazec JY. VEGF secretion by neuroendocrine tumor cells is inhibited by octreotide and by inhibitors of the PI3K/AKT/mTOR pathway. *Neuroendocrinology*. 2010;**91**(3):268–278.
47. Grunddal KV, Ratner CF, Svendsen B, Sommer F, Engelstoft MS, Madsen AN, Pedersen J, Nøhr MK, Egerod KL, Nawrocki AR, Kowalski T, Howard AD, Poulsen SS, Offermanns S, Bäckhed F, Holst JJ, Holst B, Schwartz TW. Neurotensin is coexpressed, coreleased, and acts together with GLP-1 and PYY in enteroendocrine control of metabolism. *Endocrinology*. 2016;**157**(1):176–194.
48. Bohórquez DV, Shahid RA, Erdmann A, Kreger AM, Wang Y, Calakos N, Wang F, Liddle RA. Neuroepithelial circuit formed by innervation of sensory enteroendocrine cells. *J Clin Invest*. 2015;**125**(2):782–786.
49. Marrero MB, Lucas R, Salet C, Hauser TA, Mazurov A, Lippiello PM, Bencherif M. An α7 nicotinic acetylcholine receptor-selective agonist reduces weight gain and metabolic changes in a mouse model of diabetes. *J Pharmacol Exp Ther*. 2010;**332**(1):173–180.
50. Wang X, Yang Z, Xue B, Shi H. Activation of the cholinergic antiinflammatory pathway ameliorates obesity-induced inflammation and insulin resistance. *Endocrinology*. 2011;**152**(3):836–846.
51. Mather K. Extrapancreatic effects of GLP-1 and other incretins. *Rev Endocr Metab Disord*. 2014;**15**(3):169.
52. Yamada Y, Tsukiyama K, Sato T, Shimizu T, Fujita H, Narita T. Novel extrapancreatic effects of incretin. *J Diabetes Investig*. 2016;**7**(Suppl 1):76–79.
53. Toft-Nielsen MB, Damholt MB, Madsbad S, Hilsted LM, Hughes TE, Michelsen BK, Holst JJ. Determinants of the impaired secretion of glucagon-like peptide-1 in type 2 diabetic patients. *J Clin Endocrinol Metab*. 2001;**86**(8):3717–3723.
54. Rezende LF, Vieira AS, Negro A, Langone F, Boschero AC. Ciliary neurotrophic factor (CNTF) signals through STAT3-SOCS3 pathway and protects rat pancreatic islets from cytokine-induced apoptosis. *Cytokine*. 2009;**46**(1):65–71.
55. Kappe C, Zhang Q, Holst JJ, Nyström T, Sjöholm A. Evidence for paracrine/autocrine regulation of GLP-1-producing cells. *Am J Physiol Cell Physiol*. 2013;**305**(10):C1041–C1049.
56. Wu JC, Chruscinski A, De Jesus Perez VA, Singh H, Pitsiouni M, Rabinovitch M, Utz PJ, Cooke JP. Cholinergic modulation of angiogenesis: role of the 7 nicotinic acetylcholine receptor. *J Cell Biochem*. 2009;**108**(2):433–446.
57. Xu G, Li Z, Ding L, Tang H, Guo S, Liang H, Wang H, Zhang W. Intestinal mTOR regulates GLP-1 production in mouse L cells. *Diabetologia*. 2015;**58**(8):1887–1897.